NASA TECHNICAL MEMORANDUM

NASA TM X-68169

NASA TM X-68169

EFFECT OF ROTOR DESIGN TIP SPEED ON AERODYNAMIC PERFORMANCE OF A MODEL VTOL LIFT FAN UNDER STATIC AND CROSSFLOW CONDITIONS

by N. O. Stockman, I. J. Loeffler,
and S. Lieblein
Lewis Research Center
Cleveland, Ohio

TECHNICAL PAPER proposed for presentation at
Annual Gas Turbine Conference sponsored by the
American Society of Mechanical Engineers
Washington, D.C., April 8-12, 1973

EFFECT OF ROTOR DESIGN TIP SPEED ON AERODYNAMIC PERFORMANCE OF A MODEL VTOL LIFT FAN UNDER STATIC AND CROSSFLOW CONDITIONS

by

N. O. Stockman
Aerospace Engineer

I. J. Loeffler
Aerospace Engineer

S. Lieblein
Chief, VTOL Propulsion Branch

Lewis Research Center
National Aeronautics and Space Administration
Cleveland, Ohio

E-7230

ABSTRACT

Results are presented for a wind tunnel investigation of three single VTOL lift fan stages designed for the same overall total pressure ratio at different rotor tip speeds. The stages were tested in a model lift fan installed in a wing pod. The three stages had essentially the same aerodynamic performance along the operating line. However, differences in stage thrust characteristics were obtained when a variation in back pressure was imposed on the stages by crossflow effects and thrust-vectoring louvers.

INTRODUCTION

High-bypass-ratio fans are currently considered as the most appropriate device for providing vertical lift for civil VTOL transport aircraft (ref. 1). To satisfy the requirements for efficient VTOL application, such lift fan stages must be quiet, properly matched with the drive power source, and have good performance characteristics over the entire flight range from vertical takeoff (static case) through the transition (crossflow case) to conventional flight.

One of the variables in the design of a lift fan stage of given pressure ratio is the tip speed of the rotor blades. For a given rotor total pressure ratio, there is a relatively wide range of allowable design tip speeds within prescribed blade loading limits on the rotor or stator. In general, high rotor tip speed is desirable for more efficient drive turbine performance. However, low rotor tip speed produces lower stresses, reduced gyroscopic moments, and perhaps less noise.

A test program was conducted at the NASA Lewis Research Center to investigate the effect of rotor design tip speed on the aerodynamic and noise performance of a 15-in. diameter model lift fan installed in a wing pod configuration representative of an aircraft installation. Three single fan stages were tested in which the rotors were each designed to produce an overall total pressure ratio of 1.21 at rotor tip speeds of 750, 900, and 1050 ft/sec. The investigation involved measurement of fan stage thrust and total thrust, internal flow character-

istics, and reverberant noise under static and crossflow conditions up to 160 miles per hour in the Lewis Research Center 9- by 15-foot V/STOL Propulsion Tunnel (ref. 2).

This paper presents a preliminary summary of the principal results of a comparison of the aerodynamic performance of the three single stage designs under static and crossflow conditions. Included in the comparison are operating-line performance, fan thrust maps, thrust variations with crossflow velocity, and effects of exit thrust-vectoring louvers.

APPARATUS AND DESIGN

Test Setup

The test fan stages were installed in a pod attached at mid-span to a two-dimensional wing that spanned the height of the tunnel test section, as shown in figure 1. The wing measured 4-1/2 ft. by 9 ft. with a 17 percent maximum thickness ratio. The pod was 65 in. long and 30 in. wide, with a thickness ratio of 18 percent. The fan centerline was located at the 41 percent chord point of the pod (40 percent chord point with respect to the wing). The wing could be remotely actuated through a range of angle of attack, α, of $\pm 15^{\circ}$. Maximum tunnel airflow test velocity, V_o, was around 235 ft/sec (160 mph). Further details of the wing and tunnel can be obtained in references 2, 3, and 4.

A set of five remotely-actuated louver vanes was installed at the exit of the fan to provide deflection of the exhaust flow (thrust vectoring) over a range of angle β_L from -15° (forward deflection) to +40° (aft deflection). Louver deflection angle, β_L, is defined as the angle between the chord line of the vanes and the axis of the fan. The louver vane design is the same as in reference 4. A photograph of the louver installation is shown in figure 2.

The major aerodynamic and mechanical features of the test fan assembly are illustrated in the sketch in figure 3. The fan rotor was driven by a compact two-stage supersonic turbine located within the inner casing of the assembly. The turbine was driven by high-pressure air (800 psi and 160° F) supplied through passages in the six support struts that connected the inner and outer parts of the assembly. The entire assembly was mounted on three load cells so that a measurement of axial force could be obtained. Axial separation of the rotor and stator rows was at least twice the rotor tip axial chord length. A part span damper was located at the 65 percent passage height point on the rotor blades.

The inlet bellmouth and nosepiece were axisymmetric sections with axial depth to rotor leading edge equal to 0.165 of the rotor diameter (15.0 inches). The axial depth and surface curvature were designed to minimize the possibility of local separation over the forward portion of the bellmouth at high crossflow velocities. The design was based on potential flow calculations obtained with the method described in references 5 and 6.

Pertinent test instrumentation included the following (fig. 3):

(1) Rotor inlet (station 1): wall boundary layer rakes located at the 0° and $\pm 55^{\circ}$ positions with respect to the incoming crossflow; and eight static pressure taps located 3/4 inch upstream of the rotor. The static pressures at the 3/4-inch location were used to obtain fan weight flow rate based on a correlation established from potential flow theory.

(2) Rotor outlet (station 2): six equally-spaced rakes with probes for measuring total pressure and flow angle; and six static pressure taps each on the hub and shroud surfaces.

(3) Discharge duct (station 3'): six-equally spaced rakes with elements for measuring flow angle, total pressure, and total temperature. The rakes were located halfway between the support struts. Six static pressure taps each were placed on the hub and shroud walls in the plane of the rake elements. A second set of pressure taps were located 1.2 inches further downstream (station 3).

Fan Stage Designs

The three individual single stages were designed for a nominal total pressure ratio in the discharge duct of 1.21 and a nominal corrected weight flow per unit inlet flow area of 37.2 lbs/sec ft^2. The nominal design corrected thrust per unit inlet flow area was 684 lb/ft^2. Ambient static pressure was assumed at the exit of the duct. The design average axial Mach number at the inlet to the rotor was 0.53. Design

outlet Mach number was also 0.53 with axial discharge from the stators. The hub-tip ratio at the inlet to the rotor was 0.46. Inlet flow area, A, at the rotor leading edge was 0.9868 ft^2.

Table I lists the major design characteristics of the three stage configurations. For the rotor blades, the ratio of chord length at the tip to chord length at the hub was 1.3. The corresponding taper ratio for the stator blades was 1.1. Both the rotor and stator blades had an aspect ratio of 3.1 based on average chord and span lengths. For economy, only one set of stator vanes was used, with stagger angle reset as required.

Blade-row velocity diagrams were determined from a calculation procedure involving complete radial equilibrium with a spline fit for the streamline curvature. At the inlet to the rotor, the radial flow distribution was obtained from the potential flow solution for the inlet section. Flow blockage at blade row inlet and outlet was applied uniformly to all stream tubes.

All blade sections on the rotor and stator were double circular arc profiles. Design deviation angles were based on the two-dimensional cascade correlations of reference 7 with correction factors for annular and high-speed effects. Design incidence angles were also based on the two-dimensional correlations of reference 7 with corrections for effects of relative inlet Mach number. Blade-element total pressure loss coefficients were based on blade solidity and diffusion factor with adjustments for end effects.

The principal effect of the variation in rotor design speed is the variation in aerodynamic blade loading (generally important at the tip of the rotor and the hub of the stator). For these designs, aerodynamic blade loading was described in terms of the blade-element diffusion factor (ref. 8). The calculated variation in blade-element diffusion factor across the passage at design conditions for both rotor and stator is shown in figure 4 for the three stages. The increase in design diffusion factor at both the rotor tip and the stator hub with decreasing design tip speed is clearly evident. Thus, the 750 ft/sec design can be referred to as the high-loading stage, and the 1050 ft/sec design can be called the low-loading stage.

RESULTS

One of the principal performance parameters for a lift fan is the thrust force produced by the flow through the fan stage passage. For these tests, fan stage thrust was computed from measured values of pressure, angle, and temperature in the fan duct. The drive-turbine work output as well as the fan duct thermocouples were used to establish mass-averaged total temperatures. Thrust was expressed in terms of the corrected value divided by the inlet flow area, $F/\delta A$. Performance results are presented separately for the static ($V_o = 0$) and crossflow cases.

Static Performance

Operating line. - The basic operating configuration of a lift fan is defined herein as the fan with the thrust vectoring louvers in the full open position ($\beta_L \approx 0^\circ$). For this condition, the fan duct exit is exposed to essentially ambient pressure. This represents the fan configuration for vertical takeoff, and upon which the installed thrust requirement is generally based.

The basic performance of each stage along its static operating line is shown in figure 5 as the variation of duct (overall) total pressure ratio $\overline{P}_{3'}/P_0$, corrected weight flow per unit inlet flow area $w_1\sqrt{\theta}/\delta A$, and thrust parameter $F/\delta A$ against rotor corrected tip speed $U_t/\sqrt{\theta}$. It is seen from these figures that measured performance closely matched design conditions for all three stages. Overall adiabatic efficiency was not plotted because of excessive scatter in the data. However, it appeared that the calculated efficiencies for the three stages were at about the same level (around 0.80) at design speed, and then increased with decreasing speed.

Operating range. - The operating range of a stage for lift fan application was defined as the variation of stage thrust parameter with stage back pressure ratio (ratio of stage-exit static pressure to ambient static pressure). For the configuration of this test, the average static pressure on the hub and shroud walls of the discharge duct (station 3) was taken as the measure of the fan stage back pressure. The annular area at station 3 was essentially the same as the annular area at the exit of the stators.

The operating range of each stage was determined by operation of a remotely-actuated throttling plug into an extension of the fan duct passage as shown in figure 6. The outer wall of the duct extension served as a diffuser so that below-ambient static pressures could be achieved.

Figures 7(a), (b), and (c) show the fan stage thrust maps as obtained from the throttle duct tests for the 750, 900, and 1050 ft/sec rotors, respectively. For a thrust map, stall is approached to the right (back pressure above ambient), and choke is approached to the left (back pressure below ambient). A marked difference in the thrust characteristic is observed between the low and high speed stages, particularly at the high tip speeds. Inasmuch as the 750 ft/sec stage was designed for relatively high rotor tip and stator hub loadings (fig. 4), it had a relatively small stall margin; hence the relatively rapid fall off in thrust as back pressure was increased (fig. 7(a)). On the other hand, the 1050 ft/sec stage was designed for relatively light blade loadings (fig. 4), and therefore exhibited a wide stall margin with increasing thrust as back pressure was increased (fig. 7(c)). The range of the 900 ft/sec stage, designed for medium loading, fell in between the other two (fig. 7(b)).

The dashed lines on the thrust map figures represent the variation in back pressure ratio for the stages with the louvers in the undeflected position (stage operating line). In all cases, the operating-line duct static pressures were somewhat below ambient, and decreased with increasing rotor tip speed.

The static performance characteristics of the three stages showed that essentially the same overall performance can be obtained for each of the three design rotor tip speeds along the stage operating line. However, if the fan is required to operate over a wide range of back pressure ratios, the resultant stage thrusts could be radically different. The 750 ft/sec highly-loaded stage might have a much narrower range of operation than the 1050 ft/sec lightly-loaded stage for above-ambient back pressure ratios.

Crossflow Performance

Open louvers. - Figure 8 shows a comparison of the variation of stage thrust parameter as tunnel airflow (crossflow) velocity is increased for the undeflected louver configuration at zero wing angle of attack. Two principal observations can be made. The first is that, in general, there was no large fall-off in thrust as crossflow velocity was increased. Thus, the performance of the fan stages should pose no problems for lift fan operation during transition. The second observation is an apparent divergence of the thrust variations in crossflow for the three stage designs. The thrust in crossflow for the high-loading 750 ft/sec stage was always greater than that for the low-loading 1050 ft/sec stage, with the 900 ft/sec stage falling in between. Thus, as far as open-louver performance in crossflow is concerned, fan stage performance is again acceptable, with only small differences appearing for the three rotor design tip speeds.

Deflected louvers. - Variations of fan stage thrust produced by varying the louver chord angle are shown in figure 9 for the three stages for maximum crossflow velocity and zero crossflow velocity. Data are presented for design speed and 70 percent of design speed for each stage at a wing angle of attack of zero degrees.

Two principal observations can be made about the comparative response of the three stages to louver deflection. First, the 750 ft/sec stage showed a large decrease in thrust as exhaust flow was deflected, while the trend tended to be reversed for the 1050 ft/sec stage. Second, the thrust in crossflow increased significantly over the static value for positive louver angles for the 750 ft/sec stage, but showed essentially no change for the 1050 ft/sec stage. In fact, the 750 ft/sec stage produced more stage thrust than the 1050 ft/sec stage at a crossflow velocity of 235 ft/sec up to a louver angle of 27° at design speed, and up to 34° at 70 percent design speed. The thrust characteristics of the 900 ft/sec stage were in between those of the other two stages.

Thus, if only moderate thrust deflections are required in crossflow (say, from 20° to 25°), the lower design tip speed stages (750 ft/sec and 900 ft/sec) should give good performance with these particular louvers. However, if sustained thrust is required at very large deflection angles (greater than 30° or 35°), then the higher tip speed stages (900 ft/sec and 1050 ft/sec) appear preferable.

DISCUSSION OF RESULTS

Crossflow Effects

When an aircraft containing an operating lift fan attains forward flight (crossflow case), the flow entering the fan is no longer symmetrical as in the static case. The incoming flow now has a crossflow component and must turn up to 90° to enter the inlet to the fan. Ideally, the crossflow operation should result in an increase in fan stage thrust because of the potential for converting the momentum of the approaching air to total pressure rise (ram effect). However, in reality, the crossflow orientation can tend to reduce thrust because of certain real flow effects.

Lift fan operation in crossflow is illustrated in figure 10. In crossflow, the inflow velocity is increased over the forward portion of the bellmouth and decreased over the aft portion. At the same time, the incomplete turning of the air results in an advancing/retreating blade motion with respect to the incoming air. These two factors result in a circumferential variation in angle of attack on the rotor blade. This form of inlet flow distortion is a potential flow (constant total pressure) phenomenon.

On the surfaces of the inlet bellmouth, the forward portion of the outer shroud and the aft portion of the nosepiece would experience pronounced accelerating and decelerating flows resulting from the surface curvatures. These surface velocity gradients can lead to local boundary

layer separation at the inlet to the rotor. This form of inlet distortion is a viscous flow phenomenon.

At the same time, operation in crossflow can alter the fan stage back-pressure ratio and therefore the stage operating point. The back-pressure ratio of the fan stage will vary directly with the static pressure ratio in the plane of the exit of the duct. Variations in duct-exit plane static pressure can arise from a number of general effects: (1) the conventional base pressure effect due to the discharge and diffusion of an annular jet with a blunt base (i.e., the base drag effect); (2) operation of various external devices such as louvers or spoilers which alter the direction or effective area of the exhaust flow; (3) the aerodynamic flow around the pod containing the fan; and (4) aerodynamic interactions between the fan discharge flow and the flow about the fan pod.

The base pressure effect generally results in below-ambient static pressures along the base and across the exit flow passage (e.g., ref. 3). Thrust vectoring and spoiling devices generally produce exit pressures that are greater than ambient. Aerodynamic flow effects can be either positive or negative.

All of the above phenomena (potential flow distortion, boundary layer separation, and back pressure ratio changes) can combine to produce a reduction in fan thrust compared to the ideal case as crossflow velocity is increased. The crossflow situation for lift fans is a phenomenon that has been recognized for some time. It was of interest therefore to

examine the basis of the observed effects of rotor design tip speed on the response of a lift fan stage to the inlet and outlet flow distortions induced by the crossflow operation.

Open Louvers

The crossflow characteristics of the three stages with open louvers as shown in figure 8 can be understood from examination of three principal factors: (1) the condition of the boundary layer on the inlet bellmouth at the rotor inlet; (2) the response or tolerance of the rotor row to the distortion of the inlet potential flow; and (3) changes in stage back-pressure ratio.

Inlet boundary layer. - The condition of the inlet boundary layer was determined from examination of the data from the inlet boundary layer rakes at the 0° and $\pm 55^{\circ}$ positions (fig. 3) for the three rotor speeds. At zero wing angle of attack, although there was an increase in wall boundary layer thickness as crossflow velocity increased, there was no evidence of a separated profile for any of the stages. Thus, there should be little tendency for thrust to decrease due to increased inlet total pressure loss.

Distortion tolerance. - The response of the rotor rows to the inflow distortion is illustrated in figure 11. The figure presents plots of the circumferential variation of rotor outlet total pressure ratio at mid passage for several crossflow velocities at 100 percent design speed for each of the stages. The pronounced variation in outlet total

pressure was a direct reflection of the corresponding circumferential variations in local angle of attack and velocity.* The variations were generally similar for all three rotors. However there was a tendency for the maximum total pressure rise with crossflow at 270° to be somewhat less for the 1050 ft/sec rotor than for the other two rotors. In fact, at mid radius for design speed, the ratio of the circumferentially averaged rotor outlet total pressure ratio at V_o = 235 ft/sec to the corresponding value at V_o = 0 (static case) was 0.981 for the 750 ft/sec stage, 0.979 for the 900 ft/sec stage, but 0.967 for the 1050 ft/sec rotor. This relative reduction in average rotor total pressure ratio could be eventually reflected in a relative reduction in stage discharge thrust, and contribute to the crossflow thrust divergence observed for the three stage designs in figure 8. The 1050 ft/sec rotor therefore appeared to have a somewhat more unfavorable response to crossflow inflow distortion than the 750 ft/sec rotor.

Back-pressure ratio. - Measured variations in stage back-pressure ratio with crossflow velocity are shown in figure 12 for two speed levels. In all cases, it is seen that increasing crossflow velocity resulted in a decrease in stage back-pressure ratio of about the same magnitude for all three stages. However, the level of back-pressure ratio was different for each stage design. The reduction in back-

*Examples of a comparison between inlet potential flow distortion and rotor outlet flow variations for a similar lift fan are given in reference 3. Data on measured distortions in inlet flow are presented in reference 9.

pressure ratio with crossflow is believed to be due to some interaction effect between the crossflow and the fan assembly discharge flows. The decrease in back pressure with increasing crossflow velocity was observed for all test values of fan speed, louver position, and wing angle of attack.

For crossflow situations in which there is little change in inlet loss and in inflow distortion response, as appears to be the case for the three stage designs tested, the static thrust map characteristic of the stages should provide a reasonable indication of the effects of back-pressure ratio on thrust in crossflow. According to the static thrust map for the 750 ft/sec stage shown in figure 7(a), a reduction in back-pressure ratio below the ambient value should tend to increase stage thrust. For the 900 ft/sec stage, according to figure 7(b), the stage thrust should remain about the same, while for the 1050 ft/sec stage (fig. 7(c)), the stage thrust should decrease. These thrust trends could be another principal contributor to the divergence of the crossflow thrust variations observed for the three stages in figure 8.

Deflected Louvers

Fan stage thrust in crossflow with louver deflection showed marked differences for the three stage designs (fig. 9). The higher thrust for the 750 ft/sec stage compared to the 1050 ft/sec stage in crossflow at $\beta_L \approx 0^\circ$ (undeflected configuration) has already been established in figure 8. Examination of test data indicated that when louver de-

flection was used in crossflow, there was little change in the inlet boundary layer characteristics and inflow distortion tolerance compared to the open-louver case for the three stage designs. The next factor to examine was then the possible effects of variations in stage back-pressure ratio with louver angle.

The effect of exit louvers on the fan stage back-pressure ratio is illustrated in figure 13 for the zero and maximum crossflow velocity cases. The increase in stage back-pressure ratio with louver deflection is explained as follows. Forward or aft louver deflection causes a reduction in the flow area at the exit of the louver, which requires that a drop in static pressure occur from louver inlet to exit. Since louver exit static pressure remains essentially constant at the local ambient value, the net effect of deflection is to raise the static pressure at the inlet to the louvers, i.e., at the exit of the fan duct.*

The back-pressure ratio level was somewhat different for the three stage designs, with higher back pressures occurring for the 1050 ft/sec stage than for the 750 ft/sec stage for both static and crossflow conditions. The increased separation of values at very high louver angles may be due in part to an increase in the measured difference in average duct exit Mach number between the 1050 ft/sec and 750 ft/sec rotors.

---

*The point of minimum back-pressure ratio did not occur at a louver chord angle of zero degrees for the static case because the louver vanes have some camber (i.e., zero chord angle did not correspond to zero flow deflection).

The lower levels of back-pressure ratio for the case of maximum crossflow velocity compared to the static case was the result of the discharge interaction effect in reducing back pressure that was shown in figure 12.

A similar comparison of back-pressure ratio variations with louver angle was found for the lower fan operating speeds. However, the increase in back-pressure ratio with louver deflection angle was reduced as tip speed was decreased because of the accompanying reduction in average flow Mach number entering the louvers (i.e., according to one-dimensional flow relations, the change in static pressure resulting from a change in flow area becomes smaller as inlet Mach number is reduced).

When viewed in terms of the accompanying variations of stage back-pressure ratio, the thrust trends with louver angle for both the static and crossflow conditions in figure 9 were very similar to those of the static thrust map for each stage as given in figure 7. The similarities can be readily appreciated from a comparison of figures 7(a) and 9(a) for the 750 ft/sec stage, figures 7(b) and 9(b) for the 900 ft/sec stage, and figures 7(c) and 9(c) for the 1050 ft/sec stage. In relating louver angle to back-pressure ratio in figure 7, it should be noted that both forward and aft louver deflection increased the back-pressure ratio.

It appears, therefore, that back-pressure ratio change was the primary factor in determining the individual stage thrust variations with louver deflection shown in figure 9. These results provide additional confirmation for the earlier hypothesis that when inlet losses and rotor inlet distortion effects are relatively small, the static thrust map can

provide a qualitative indication of thrust variations in crossflow, providing the crossflow back-pressure ratio variations are known.

Qualifications

The data presented herein were restricted to a pod configuration at zero wing angle of attack. Preliminary analysis of data taken at varying angle of attack indicated that fan stage thrust in crossflow tended to decrease somewhat with increasing angle of attack due to the less favorable inflow orientation. In fact, bellmouth flow separation started to appear at $\alpha = 15^{\circ}$ for the maximum crossflow velocities.

It should be pointed out that the fan stage thrust presented by these results is the thrust capability of the flow at the discharge of the fan duct. When louvers are present, the actual resultant thrust delivered by the fan assembly will depend on the thrust losses introduced by the louver vanes. In general, louver thrust losses increase with increasing deflection.

It should also be noted that the crossflow thrust variations of a lift fan will depend on the back pressure variations imposed by the specific configuration of the fan assembly and the attached exhaust device (for thrust deflection or spoiling). For example, a different louver vane concept or attachment arrangement could produce a different magnitude of back-pressure ratio for the same amount of thrust deflection.

SUMMARY OF RESULTS

Wind tunnel tests were conducted on a model VTOL lift fan-in-pod for which rotors were designed to produce the same stage total pressure ratio at three different design tip speeds. The major results obtained from the tests were as follows:

(1) All three stages produced essentially the same overall performance along their operating lines with open exit louvers under static (zero crossflow) conditions.

(2) The variation of static stage thrust with back-pressure ratio (static thrust map) was significantly different for the three stages. These differences were attributed to the differences in design-point blade loading. The 750 ft/sec rotor stage, with high blade loadings, had a relatively small stall margin and a pronounced fall-off in thrust with increasing back-pressure ratio. The 1050 ft/sec rotor stage, with low blade loadings, had a wide stall margin and a more favorable thrust variation with increasing back-pressure ratio.

(3) Crossflow operation had little effect on the general level of the stage thrust for the undeflected louver configuration. However, there were differences in the thrust variation with crossflow velocity for the three stage designs. The 750 ft/sec stage tended to give a somewhat higher thrust than the 1050 ft/sec stage in crossflow.

(4) Exit louver deflection in crossflow tended to produce stage thrust variations for each stage design that were similar to the individual variations of static thrust with back-pressure ratio. Because

of the back pressure effects, the lower design tip speed stages showed more favorable thrust variation for moderate louver deflection angles, while the higher tip speed designs appeared better for very large deflection angles.

REFERENCES

1. Lieblein, S., "A Review of Lift Fan Propulsion Systems for Civil VTOL transports," Paper 70-670, June 1970, AIAA, New York, N. Y.

2. Yuska, J. A., Diedrich, J. D., and Clough, N., "Lewis 9- by 15-Foot V/STOL Wind Tunnel," TM X-2305, 1971, NASA, Cleveland, Ohio.

3. Lieblein, S., Yuska, J. A., and Diedrich, J. H., "Wind Tunnel Tests of a Wing-Installed Model VTOL Lift Fan with Coaxial Drive Turbine," Paper 71-742, June 1971, AIAA, New York, N. Y.

4. Yuska, J. A. and Diedrich, J. H., "Fan and Wing Force Data from Wind-Tunnel Investigation of a 0.38-Meter (15-in.) Diameter VTOL Model Lift Fan Installed in a Two-Dimensional Wing," TN D-6654, 1972, NASA, Cleveland, Ohio.

5. Stockman, No. O. and Lieblein, S., "Theoretical Analysis of Flow in VTOL Lift Fan Inlets Without Crossflow," TN D-5065, 1969, NASA, Cleveland, Ohio.

6. Stockman, N. O., "Potential Flow Solutions for Inlets of VTOL Lift Fans and Engines," Analytic Methods in Aircraft Aerodynamics, SP-228, 1970, NASA, Washington, D.C., pp. 659-681.

7. Lieblein, S., "Experimental Flow in Two-Dimensional Cascades," Aerodynamic Design of Axial-Flow Compressors, SP-36, 1965, NASA, Washington, D.C., pp. 183-226.

8. Lieblein, S., Schwenk, F. C., and Broderick, R. L., "Diffusion Factor for Estimating Losses and Limiting Blade Loadings in Axial-Flow-Compressor Blade Elements," RM E53D01, 1953, NACA, Cleveland, Ohio.

9. Cockshutt, E. P., "VTOL Propulsion - 1970 Perspective," Canadian Aeronautics and Space Journal, Vol. 17, No. 4, Apr. 1971, pp. 117-130.

TABLE I. - FAN STAGE DESIGN VALUES UNSHROUDED ROTORS; 1.21 PRESSURE RATIO

Features	Low tip speed high loading	Medium tip speed medium loading	High tip speed low loading
ROTOR			
Corrected tip speed, ft/sec	750	900	1050
Relative tip inlet Mach no.*	0.88	0.99	1.10
Number of blades	37	37	34
Tip solidity	1.1	1.1	1.0
Tip diffusion factor*	0.41	0.34	0.32
Maximum tip thickness/chord	0.05	0.05	0.04
Maximum hub thickness/chord	0.08	0.08	0.08
STATOR			
Relative hub inlet Mach no.*	0.68	0.62	0.59
Number of blades	42	42	36
Tip solidity	1.1	1.1	0.94
Hub diffusion factor*	0.42	0.33	0.29
Stagger angle reset, deg.	+3	0	-2.5
Maximum tip thickness/chord	0.07	0.07	0.07
Maximum hub thickness/chord	0.06	0.06	0.06
Stage efficiency	0.86	0.86	0.83
Rotor-stator axial spacing**	2.3	2.8	3.1

*At 5 percent of span from wall.

**In projected rotor tip chords.

FIGURE CAPTIONS

Fig. 1. Fifteen-inch fan-in-pod model installed in the Lewis Research Center 9- by 15-foot V/STOL propulsion test section.

Fig. 2. Exit louver installation on 15-inch fan-in-pod model.

Fig. 3. Cross section of 15-inch model lift fan.

Fig. 4. Radial variation of diffusion factor for 1.2 pressure ratio fan designs.

Fig. 5. Comparison of stage performance along fan static operating line. Louver angle, $\beta_L = 0.5^\circ$; wing angle of attack, $\alpha = 0^\circ$.

(a) Overall total pressure ratio.

(b) Inlet weight flow.

(c) Thrust.

Fig. 6. Remotely-actuated throttle plug for fan performance map.

Fig. 7. Fan stage static thrust map obtained from throttle duct tests.

(a) Stage with 750 ft/sec rotor.

(b) Stage with 900 ft/sec rotor.

(c) Stage with 1050 ft/sec rotor.

Fig. 8. Variation of fan stage thrust with crossflow velocity for undeflected louvers. Louver angle, $\beta_L = 0.5^\circ$; wing angle, $\alpha = 0^\circ$.

Fig. 9. Effect of louver angle on fan stage thrust in crossflow. Wing angle, $\alpha = 0^\circ$.

(a) Stage with 750 ft/sec rotor.

(b) Stage with 900 ft/sec rotor.

(c) Stage with 1050 ft/sec rotor.

Fig. 10. Lift fan inflow in crossflow.

Fig. 11. Circumferential variation of rotor outlet total pressure ratio in crossflow. Mid radius position; design speed for each rotor. Louver angle, $\beta_L = 0.5^\circ$; wing angle, $\alpha = 0^\circ$.

Fig. 12. Fan stage back pressure in crossflow. Louver angle, $\beta_L = 0.5^\circ$; wing angle, $\alpha = 0^\circ$.

Fig. 13. Effect of louver angle on fan stage back-pressure ratio. Rotor tip speed, 100 percent design; wing angle, $\alpha = 0^\circ$.

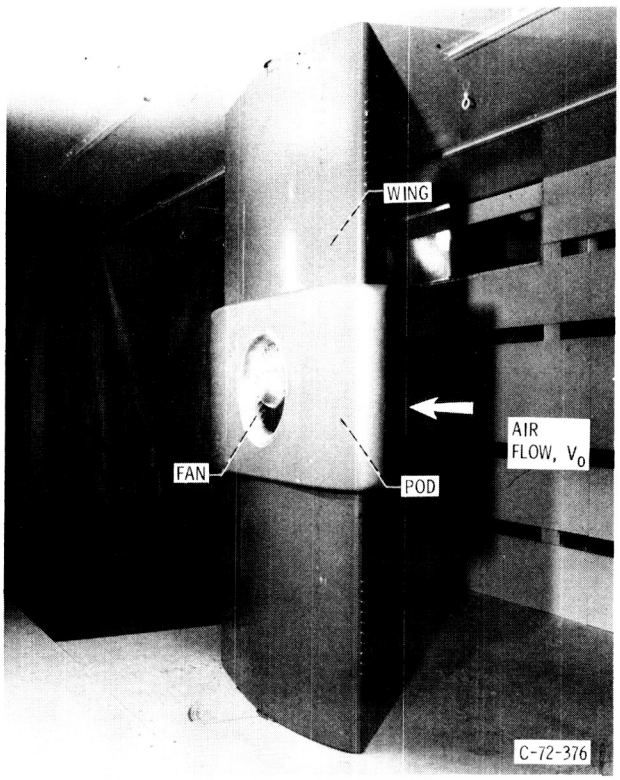

Figure 1. - Fifteen-inch fan-in-pod model installed in the Lewis Research Center 9- by 15-foot V/STOL propulsion test section.

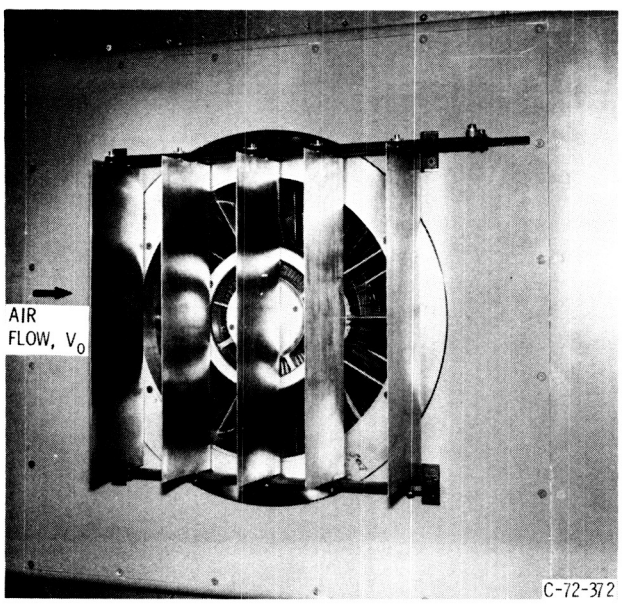

Figure 2. - Exit louver installation on 15-inch fan-in-pod model.

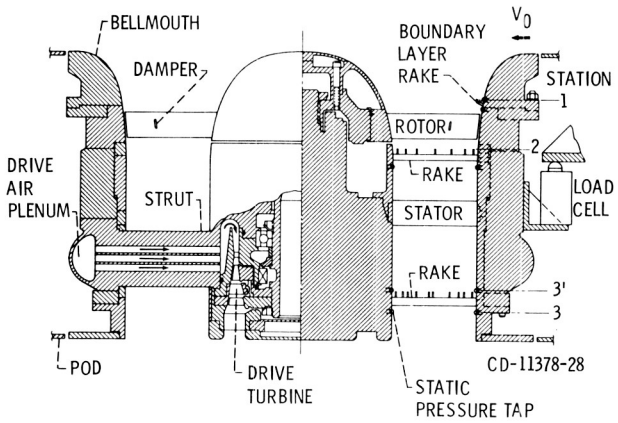

Figure 3. - Cross section of 15-inch model lift fan.

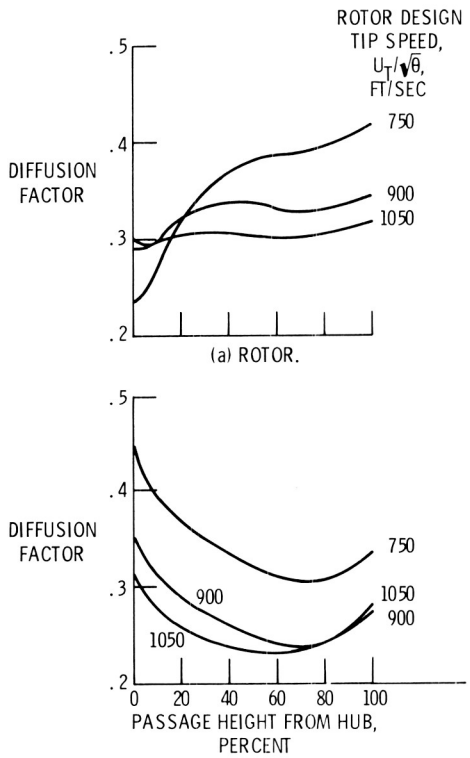

Figure 4. - Radial variation of diffusion factor for 1.2 pressure ratio fan designs.

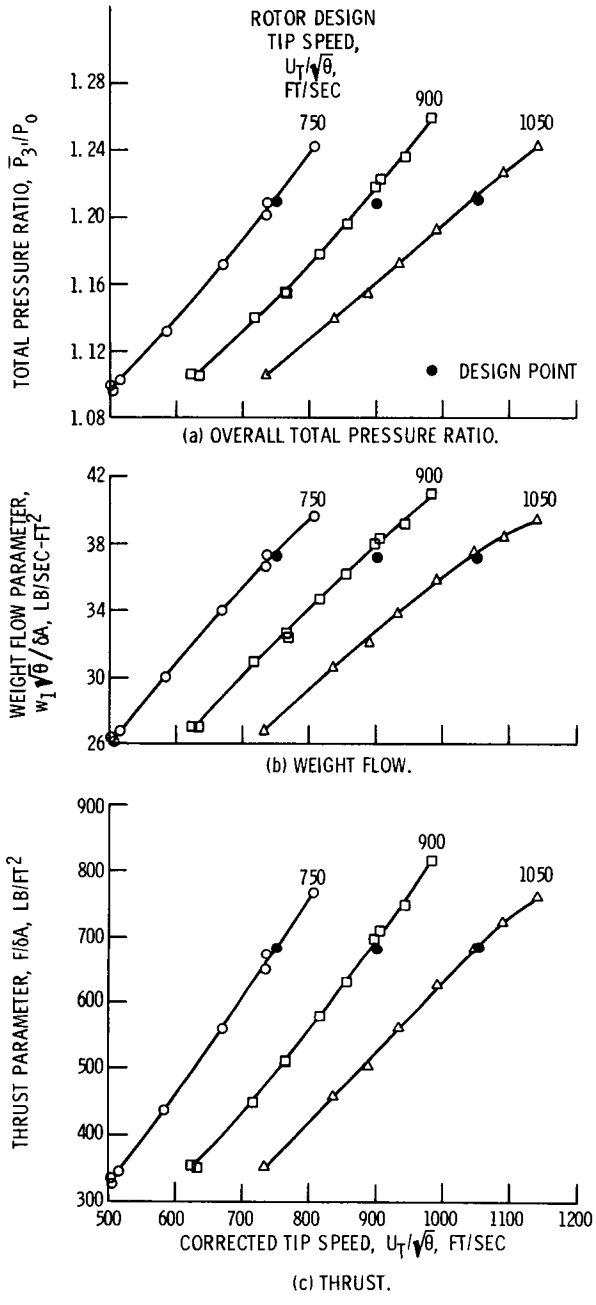

Figure 5. - Comparison of stage performance along fan static operating line. Louver angle, $\beta_L = 0.5^o$; wing angle of attack, $\alpha = 0^o$.

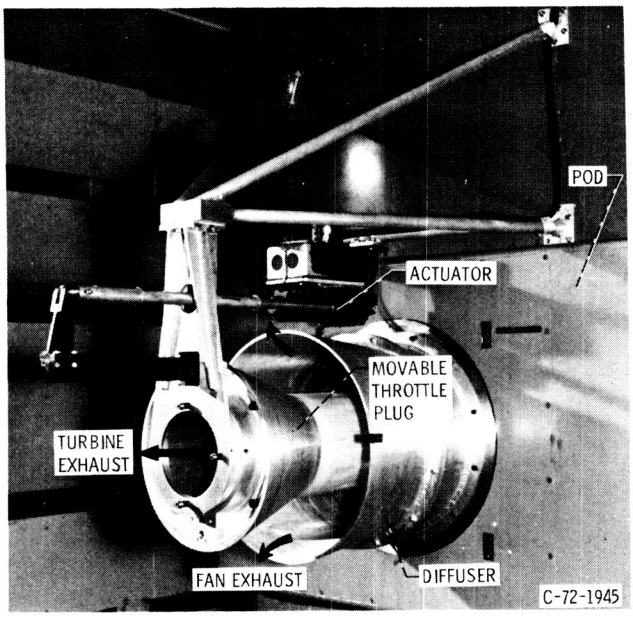

Figure 6. - Remotely actuated throttle plug for fan performance map.

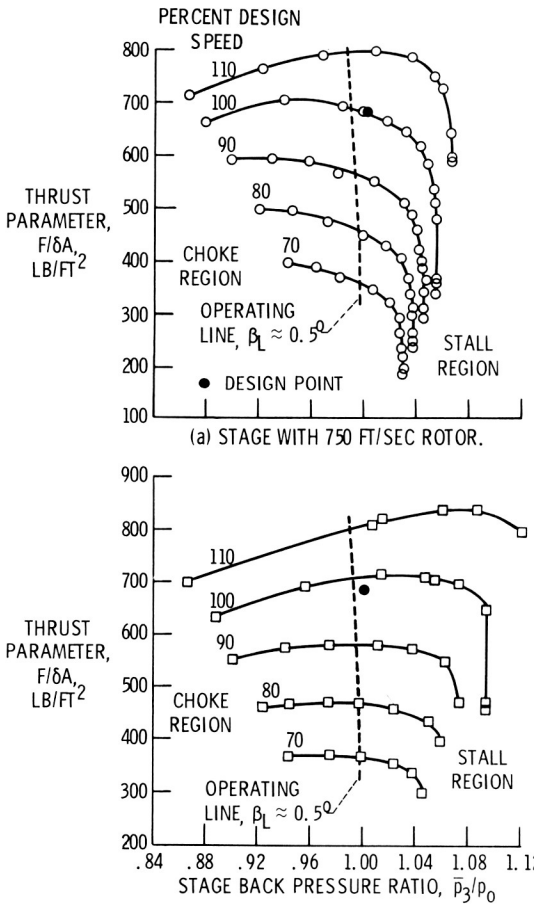

Figure 7. - Fan stage static thrust map obtained from throttle duct tests.

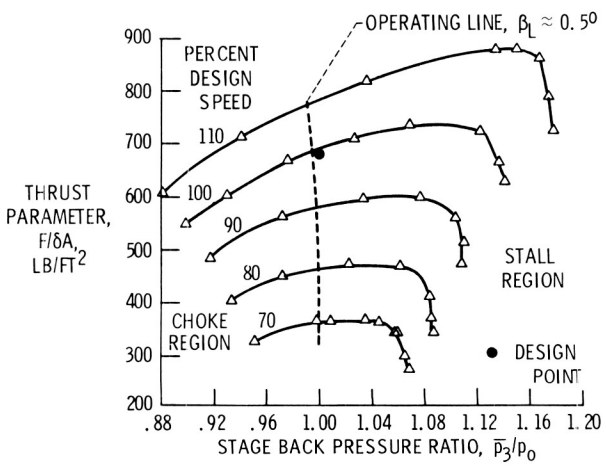

Figure 7. - Concluded.

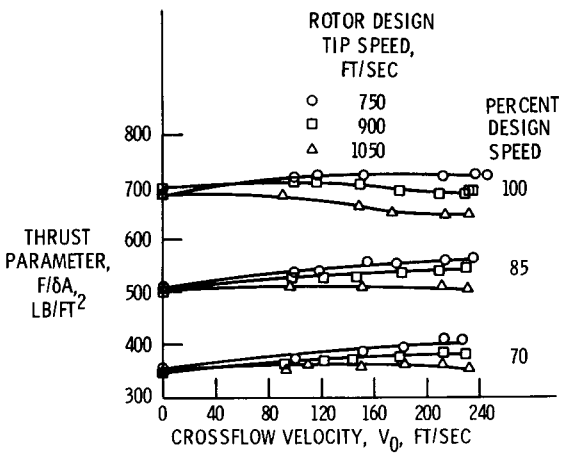

Figure 8. - Variation of fan stage thrust with crossflow velocity for undeflected louvers. Louver angle, $\beta_L = 0.5^0$; wing angle, $\alpha = 0^0$.

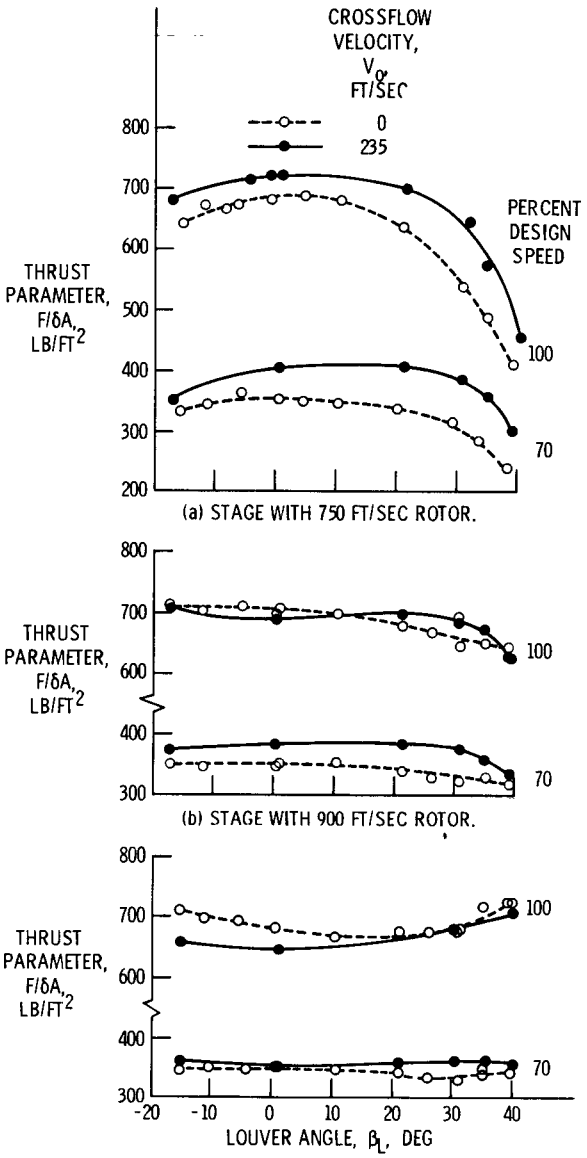

Figure 9. - Effect of louver angle on fan stage thrust in crossflow. Wing angle, $\alpha = 0^0$.

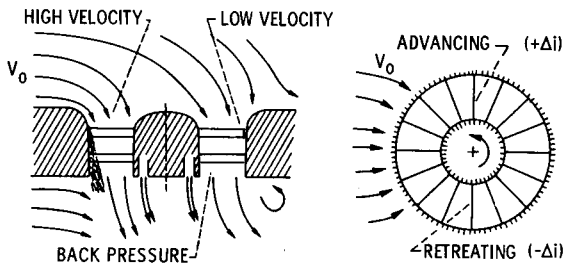

Figure 10. - Lift fan inflow in crossflow.

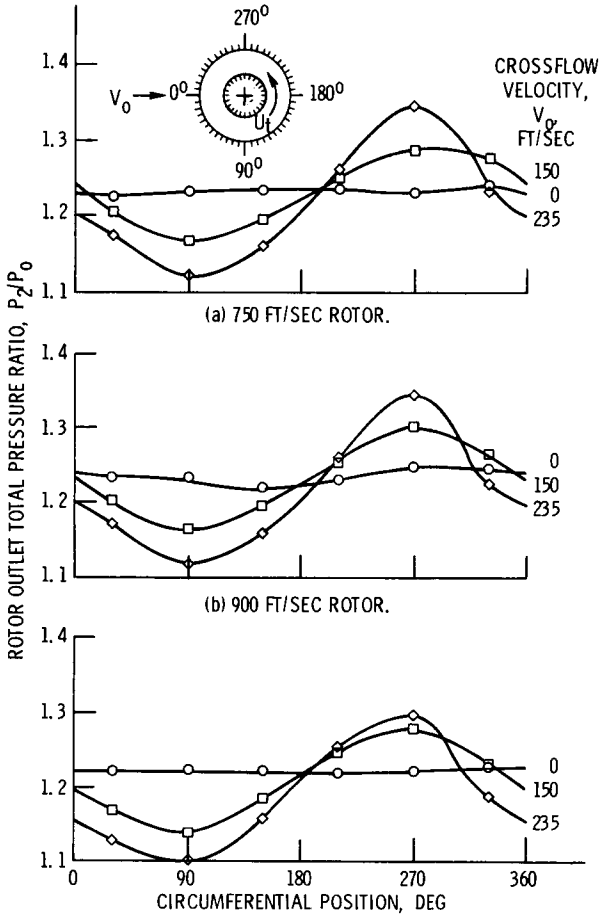

Figure 11. - Circumferential variation of rotor outlet total pressure ratio in crossflow. Midradius position; design speed for each rotor. Louver angle, $\beta_L = 0.5^0$; wing angle, $\alpha = 0^0$.

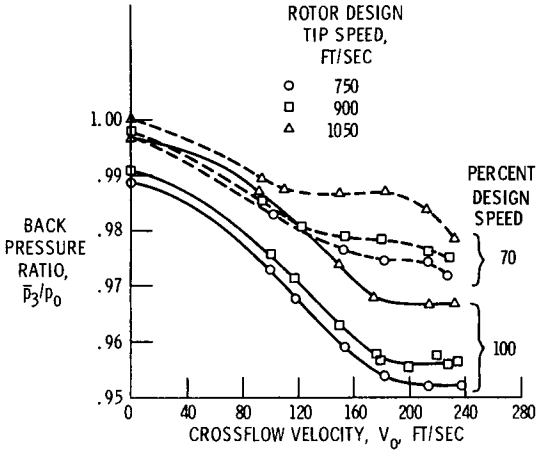

Figure 12. - Fan stage back pressure in crossflow. Louver angle, $\beta_L = 0.5^0$; wing angle, $\alpha = 0^0$.

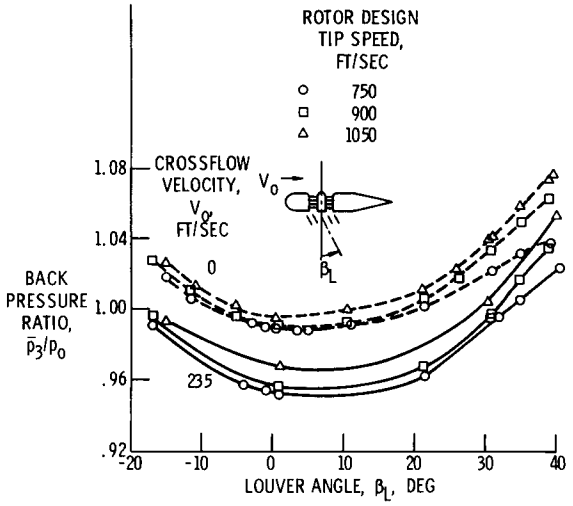

Figure 13. - Effect of louver angle on fan stage back pressure ratio. Rotor tip speed, 100 percent design; wing angle, $\alpha = 0^0$.